Volkan Yıldız, Mehmet Pakdemirli* and Yiğit Aksoy

Parallel Plate Flow of a Third-Grade Fluid and a Newtonian Fluid With Variable Viscosity

Abstract: Steady-state parallel plate flow of a third-grade fluid and a Newtonian fluid with temperature-dependent viscosity is considered. Approximate analytical solutions are constructed using the newly developed perturbation-iteration algorithms. Two different perturbation-iteration algorithms are used. The velocity and temperature profiles obtained by the iteration algorithms are contrasted with the numerical solutions as well as with the regular perturbation solutions. It is found that the perturbation-iteration solutions converge better to the numerical solutions than the regular perturbation solutions, in particular when the validity criteria of the regular perturbation solution are not satisfied. The new analytical approach produces promising results in solving complex fluid problems.

Keywords: Parallel Plate Flow; Perturbation Methods; Perturbation-Iteration Algorithms; Reynolds Model; Third-Grade Fluids.

1 Introduction

Perturbation methods [1] have been used widely in an attempt to obtain analytical solutions for differential equations, algebraic equations, etc. However, these methods have a drawback which is the small parameter requirement and as a consequence, the solutions become only valid for weak nonlinearities. Eventually, some studies have been carried out to overcome this drawback. A few of them are the modified Lindstedt-Poincare method [2], the multiple-scales Lindstedt-Poincare method [3], the artificial parameter method [4], and the variational iteration method [5].

A different approach to obtain valid solutions for strong nonlinear systems is the iterative perturbation techniques [6–10]. In these techniques, some initial assumptions and special transformations need to be made before the iteration procedure. A new and more systematic iterative perturbation method called "the perturbation-iteration algorithm" that does not require initial assumptions and special transformations has been developed [11]. The new perturbation-iteration algorithm is based on the perturbation-iteration algorithms developed for algebraic equations [12–14]. This new iterative method has been successfully applied to Bratu-type equations [15] and some nonlinear heat transfer equations [16]. It has also been applied to Fredholm and Volterra integral equations [17] as well as to the first-order differential systems [18]. Lately, the method has been applied to strongly nonlinear vibrations [19] and to boundary-layer-type problems [20].

In this article, one of the fundamental fluid flow problem, namely the parallel plate flow, is considered. The third-grade fluid, which belongs to the Rivlin-Ericksen class, is taken as the non-Newtonian model. The model can predict the shear thinning or shear thickening behaviour as well as the normal stresses which are characteristics of a typical non-Newtonian fluid. For some previous work on the topic, see [21, 22]. Classical perturbation methods are used in the mentioned work. Hence, the solutions are valid only for a combination of the small physical parameters such as the pressure drop, non-Newtonian parameter, and the Brinkman number. For a partial list of the previous work on analytical and numerical solutions of the third-grade fluids for special flow geometries, see [23–30] for example.

In this work, the newly developed perturbation-iteration algorithm is employed to increase the range of validity of the analytical solutions. A close match between the analytical and numerical solutions can be achieved by the new method for which the classical perturbation methods yield unphysical results such as back-flow adjacent to the walls or throughout the whole domain. The perturbation-iteration algorithms are classified as PIA(n,m), n representing the number of the correction terms in the perturbation expansion and m representing the degree of the highest order derivative in the Taylor Series expansions [11–20]. Two different perturbation-iteration algorithms namely the PIA(1,1) and PIA(1,2) are employed and the results of the different algorithms are contrasted with

---

*Corresponding author: Mehmet Pakdemirli, Applied Mathematics and Computation Center, Celal Bayar University, Muradiye, Manisa, Turkey, Tel.: +90(236)2012040, E-mail: mpak@cbu.edu.tr
Volkan Yıldız and Yiğit Aksoy: Department of Mechanical Engineering, Celal Bayar University, Muradiye, Manisa, Turkey

the numerical and classical perturbation solutions. As a general rule, PIA(1,2) performs better than PIA(1,1) with exceptions.

As a second problem, a Newtonian fluid with temperature-dependent viscosity according to the Reynolds model is considered. Due to the dependence of exponentially decaying viscosity on the temperature, the governing equations become highly nonlinear and coupled. The iteration procedure enables uncoupling of the momentum and energy equations, and hence, construction of the solutions becomes easier. Results of the PIA(1,1) and the PIA(1,2) are then compared with the regular perturbation and the numerical solutions. It is found that the PIA(1,1) solutions are more reliable and straightforward due to the termination of the iterations and limitation of the logarithmic function appearing in the PIA(1,2) case.

2 Perturbation-Iteration Algorithms

An infinite number of different perturbation-iteration algorithms can be developed in theory for both algebraic and differential equations [11–20]. The algorithms were named as PIA(n,m), where n is the number of correction terms in the perturbation expansion and m is the highest order of derivative in the Taylor series expansion. n should always be less than or equal to m for the equations to be solvable. As n and m increases, the complexity of the iteration equations increases, yielding highly nonlinear coupled equations which are unsolvable analytically. Hence, it is logical to take only a few terms, and in this study, PIA(1,1) and PIA(1,2) are employed in search of analytical solutions.

2.1 Perturbation-Iteration Algorithm PIA(1,1) for Second-Order Coupled Differential Equations

The problems investigated are second-order nonlinear equations with coupling between the velocity and temperature. Hence, the theory is presented for such equations. The simplest iteration algorithm is the PIA(1,1) algorithm which is constructed by taking one correction term in the perturbation expansion and only the first-order derivate terms in the Taylor series expansion. For the general nonlinear second-order ordinary differential equations with two dependent variables

$$F_1(u'', u', u, \theta'', \theta', \theta, \varepsilon)=0, \qquad (1)$$

$$F_2(u'', u', u, \theta'', \theta', \theta, \varepsilon)=0, \qquad (2)$$

where both u and θ are functions of y, $u=u(y)$, $\theta=\theta(y)$, y being the coordinate vertical to the plates and ε is the perturbation parameter. If the equations do not possess a perturbation parameter, it can be inserted artificially. Broadly speaking, the perturbation parameter is usually inserted as a coefficient in front of the nonlinear terms. Taking just one correction term in the perturbation expansion

$$u_{n+1}=u_n+\varepsilon(u_c)_n, \qquad (3)$$

$$\theta_{n+1}=\theta_n+\varepsilon(\theta_c)_n. \qquad (4)$$

Substituting (3) and (4) into (1) and (2), and expanding them in a Taylor series with first-order derivatives leads to

$$F_i=F_i\Big|_{\varepsilon=0}+\frac{DF_i}{D\varepsilon}\Big|_{\varepsilon=0} \varepsilon=0 \quad i=1, 2, \qquad (5)$$

where the total derivative is defined as

$$\frac{D}{D\varepsilon}=\frac{\partial}{\partial\varepsilon}+\frac{\partial}{\partial u''}\frac{\partial u''}{\partial\varepsilon}+\frac{\partial}{\partial u'}\frac{\partial u'}{\partial\varepsilon}+\frac{\partial}{\partial u}\frac{\partial u}{\partial\varepsilon}+\frac{\partial}{\partial\theta''}\frac{\partial\theta''}{\partial\varepsilon}$$
$$+\frac{\partial}{\partial\theta'}\frac{\partial\theta'}{\partial\varepsilon}+\frac{\partial}{\partial\theta}\frac{\partial\theta}{\partial\varepsilon}, \qquad (6)$$

and evaluated at $\varepsilon=0$. Note that in this method, the dependent variables and their derivatives are considered to be independent of each other. Their contributions to the total derivative are calculated separately and added to each other as shown in (6). Using (5), one will have two coupled equations of $(u_c)_n$ and $(\theta_c)_n$ to be solved in order. With two initial guesses, u_0 and θ_0, which satisfy the boundary conditions, $(u_c)_0$ and $(\theta_c)_0$ can be calculated and later substituted into (3) and (4) to calculate u_1 and θ_1. This iteration procedure can be repeated until satisfactory results are obtained.

2.2 Perturbation-Iteration Algorithm PIA(1,2) for Second-Order Coupled Differential Equations

In this iteration algorithm, only one correction term in the perturbation expansion is taken and up to second-order derivatives in the Taylor series expansion are included, i.e. $n=1$, $m=2$. The algorithm is named as PIA(1,2). Again, the perturbation expansions with one correction terms

$$u_{n+1}=u_n+\varepsilon(u_c)_n \qquad (7)$$

$$\theta_{n+1}=\theta_n+\varepsilon(\theta_c)_n \qquad (8)$$

are substituted into (1) and (2) and expanded in a Taylor series up to second-order derivatives leading to

$$F_i = F_i \mid_{\varepsilon=0} + \frac{DF_i}{D\varepsilon} \mid_{\varepsilon=0} \varepsilon + \frac{1}{2} \frac{D^2F_i}{D\varepsilon^2} \mid_{\varepsilon=0} \varepsilon^2 = 0 \quad i=1, 2. \tag{9}$$

One will have two differential equations in terms of the unknowns $(u_c)_n$ and $(\theta_c)_n$ again, which have to be solved and substituted into (7) and (8). The iterative procedure is set up in the same way as explained for the PIA(1,1).

3 Parallel Plate Flow of a Third-Grade Fluid

Consider the steady-state flow of a third-grade fluid between parallel plates with heat transfer. The non-dimensional form of the equations of motion was derived by Szeri and Rajagopal [21]

$$\mu\left(\frac{d^2u}{dy^2}\right) + 6\varepsilon\Lambda\left(\frac{du}{dy}\right)^2 \frac{d^2u}{dy^2} = C \quad u(0)=0, \ u(1)=0, \tag{10}$$

$$\frac{d^2\theta}{dy^2} + \Gamma\mu\left(\frac{du}{dy}\right)^2 + 2\varepsilon\Lambda\Gamma\left(\frac{du}{dy}\right)^4 = 0 \quad \theta(0)=0, \ \theta(1)=1, \tag{11}$$

where u is the dimensionless velocity, θ is the dimensionless temperature, and μ is the dimensionless viscosity. The terms are related to the dimensional (with over tilde) parameters through the following relations:

$$y=\frac{\tilde{y}}{h}, \ \theta=\frac{\tilde{\theta}-\theta_1}{\theta_2-\theta_1}, \ u=\frac{\tilde{u}}{V}, \ \mu=\frac{\tilde{\mu}}{\mu_*}, \tag{12}$$

where h is the distance between the parallel plates, θ_1 and θ_2 are the lower and upper plate temperatures, respectively, V is the reference velocity, and μ_* is the reference viscosity. The dimensionless parameters involved in (10) and (11) are

$$C=\frac{C_1h^2}{\mu_*V}, \ C_1=\frac{dp}{dx}, \ \Gamma=\frac{\mu_*V^2}{k(\theta_2-\theta_1)}, \ \Lambda=\frac{\beta V^2}{\mu_*h^2}, \tag{13}$$

where C_1 is the constant pressure drop in the axial direction, Γ is the Brinkman number, Λ is the dimensionless parameter related to the non-Newtonian behaviour, and β is the dimensional material constant which is the coefficient of the last term in the stress-constitutive relation for a third-grade fluid

$$\mathbf{T} = -p\mathbf{I} + \mu\mathbf{A_1} + \alpha_1\mathbf{A_2} + \alpha_2\mathbf{A_1^2} + \beta(tr\mathbf{A_1^2})\mathbf{A_1}, \tag{14}$$

where $\mathbf{A_1}$ and $\mathbf{A_2}$ are the Rivlin-Ericksen tensors [21], k is the thermal conductivity of the fluid, α_1 and α_2 are the material constants, and p is the pressure. The term β can be determined if the relationship between the stress and the Rivlin-Ericksen tensor of the fluid is known. The problem will be solved using the PIA(1,1) and PIA(1,2) algorithms as well as the regular perturbation method.

3.1 Perturbation-Iteration Algorithm PIA(1,1)

If the reference viscosity is selected as the Newtonian viscosity, $\mu=1$ for the constant viscosity case. Applying the constant viscosity, (10) and (11) are rewritten in the following form:

$$F_1(u'', u', \varepsilon) = u'' + 6\varepsilon\Lambda(u')^2u'' - C = 0, \tag{15}$$

$$F_2(\theta'', u', \varepsilon) = \theta'' + \Gamma(u')^2 + 2\varepsilon\Lambda\Gamma(u')^4 = 0, \tag{16}$$

where ε is an artificially introduced small parameter. Substituting the perturbation expansions (3) and (4) into (15) and (16), then expanding in Taylor series with first-order derivatives (5) and rearranging yields

$$(u_c'')_n + \frac{u_n''}{\varepsilon} + 6\Lambda\left(u_n'\right)^2 u_n'' - \frac{C}{\varepsilon} = 0, \tag{17}$$

$$(\theta_c'')_n + 2\Gamma u_n'(u_c')_n + \frac{\theta_n''}{\varepsilon} + \frac{\Gamma(u_n')^2}{\varepsilon} + 2\Lambda\Gamma(u_n')^4 = 0. \tag{18}$$

Starting with the initial functions that satisfy the boundary conditions

$$u_0 = 0, \tag{19}$$

$$\theta_0 = y, \tag{20}$$

and using (17), (18), (3) and (4), one will obtain the first iteration solutions as follows:

$$u_1 = \frac{C}{2}(y^2 - y), \tag{21}$$

$$\theta_1 = y. \tag{22}$$

Proceeding in the same way, the subsequent iterations are

$$u_2 = \frac{C}{2}(y^2-y) + \varepsilon\Lambda C^3\left(-\frac{y^4}{2} + y^3 - \frac{3y^2}{4} + \frac{y}{4}\right), \tag{23}$$

$$\theta_2 = y + \varepsilon\Lambda\Gamma C^4\left(\frac{y^6}{15} - \frac{y^5}{5} + \frac{y^4}{4} - \frac{y^3}{6} + \frac{y^2}{16} - \frac{y}{80}\right)$$

$$+ \frac{\Gamma C^2}{4}\left(-\frac{y^4}{3} + \frac{2y^3}{3} - \frac{y^2}{2} + \frac{y}{6}\right), \tag{24}$$

$$u_3 = \frac{C}{2}(y^2 - y) + \varepsilon\Lambda C^3\left(-\frac{y^4}{2} + y^3 - \frac{3y^2}{4} + \frac{y}{4}\right)$$

$$+ \varepsilon^2 C^5\Lambda^2\left(2y^6 - 6y^5 + \frac{15y^4}{2} - 5y^3 + \frac{15y^2}{8} - \frac{3y}{8}\right)$$

$$+ \varepsilon^3 C^7\Lambda^3\left(-3y^8 + 12y^7 - 21y^6 + 21y^5 - \frac{105y^4}{8} + \frac{21y^3}{4} - \frac{21y^2}{16} + \frac{3y}{16}\right)$$

$$+ \varepsilon^4 C^9\Lambda^4\left(\frac{8y^{10}}{5} - 8y^9 + 18y^8 - 24y^7 + 21y^6 - \frac{63y^5}{5} + \frac{21y^4}{4}\right.$$

$$\left. - \frac{3y^3}{2} + \frac{9y^2}{32} - \frac{y}{32}\right), \tag{25}$$

$$\theta_3 = y + \varepsilon\Lambda\Gamma C^4\left(\frac{y^2}{15} - \frac{y^5}{5} + \frac{y^4}{4} - \frac{y^3}{6} + \frac{y^2}{16} - \frac{y}{80}\right)$$

$$+ \frac{\Gamma C^2}{4}\left(-\frac{y^4}{3} + \frac{2y^3}{3} - \frac{y^2}{2} + \frac{y}{6}\right)$$

$$+ 3\varepsilon^2 C^6\Gamma\Lambda^2\left(\frac{y^8}{14} - \frac{2y^7}{7} + \frac{y^6}{2} - \frac{y^5}{2} + \frac{5y^4}{16} - \frac{y^3}{8} + \frac{y^2}{32} - \frac{y}{224}\right)$$

$$+ \varepsilon^3 C^8\Gamma\Lambda^3\left(-\frac{8y^{10}}{15} + \frac{8y^9}{3} - 6y^8 + 8y^7 - 7y^6 + \frac{21y^5}{5}\right.$$

$$\left. - \frac{7y^4}{4} + \frac{y^3}{2} - \frac{3y^2}{32} + \frac{y}{96}\right)$$

$$+ \varepsilon^4 C^{10}\Gamma\Lambda^4\left(\frac{16y^{12}}{33} - \frac{32y^{11}}{11} + 8y^{10} - \frac{40y^9}{3} + 15y^8 - 12y^7\right.$$

$$\left. + 7y^6 - 3y^5 + \frac{15y^4}{16} - \frac{5y^3}{24} + \frac{y^2}{32} - \frac{y}{352}\right)$$

$$+ \varepsilon^5 C^{12}\Gamma\Lambda^5\left(-\frac{16y^{14}}{91} + \frac{16y^{13}}{13} - 4y^{12} + 8y^{11} - 11y^{10} + 11y^9 - \frac{33y^8}{4}\right.$$

$$\left. + \frac{33y^7}{7} - \frac{33y^6}{16} + \frac{11y^5}{16} - \frac{11y^4}{64} + \frac{y^3}{32} - \frac{y^2}{256} + \frac{y}{3328}\right). \tag{26}$$

Note that the solutions are of polynomial type for this specific algorithm and becomes lengthy as the number of iterations increase.

3.2 Perturbation-Iteration Algorithm PIA(1,2)

For this case, the problem will be solved using the perturbation-iteration algorithm PIA(1,2). Substituting the perturbation expansions (7) and (8) into (15) and (16), then expanding in Taylor series up to second-order derivatives (9), the iteration formulas for the PIA(1,2) reduces to

$$u_n'' - C + 6\varepsilon\Lambda(u_n')^2 u_n'' + \varepsilon(u_c'')_n + 12\varepsilon^2\Lambda u_n' u_n''(u_c')_n$$

$$+ 6\varepsilon^2\Lambda(u_n')^2(u_c'')_n = 0, \tag{27}$$

$$\theta_n'' + \Gamma(u_n')^2 + 2\varepsilon\Lambda\Gamma(u_n')^4 + \varepsilon(\theta_c'')_n + 2\varepsilon\Gamma u_n'(u_c')_n$$

$$+ 8\varepsilon^2\Lambda\Gamma(u_n')^3(u_c')_n + \varepsilon^2\Gamma(u_c')_n^2 = 0. \tag{28}$$

With the initial choices

$$u_0 = 0, \tag{29}$$

$$\theta_0 = y, \tag{30}$$

the first and the second iteration solutions are

$$u_1 = \frac{C}{2}(y^2 - y), \tag{31}$$

$$\theta_1 = y + \frac{\Gamma C^2}{4}\left(-\frac{y^4}{3} + \frac{2y^3}{3} - \frac{y^2}{2} + \frac{y}{6}\right), \tag{32}$$

$$u_2 = \frac{C}{2}(y^2 - y) + \frac{1}{72\varepsilon C\Lambda}\{2(\ln[2 + 3\varepsilon\Lambda C^2(2y - 1)^2]$$

$$- \ln[2 + 3\varepsilon C^2\Lambda]) + 12\varepsilon C^2\Lambda(y - y^2)\}. \tag{33}$$

For the sake of brevity, the lengthy solution calculated for θ_2 using a symbolic manipulation program is not written here. The PIA(1,2) generated more complex solutions in functional forms as compared to the polynomial form solutions of the PIA(1,1).

3.3 Perturbation Solution

This particular problem was solved using regular perturbation methods with one correction term by Yürüsoy, Pakdemirli, and Yilbas [22]. The solutions they found under constant viscosity assumption are

$$u = \frac{C}{2}(y^2 - y) - \frac{3}{2}\Lambda C^3\left(\frac{y^4}{3} - \frac{2y^3}{3} + \frac{y^2}{2} - \frac{y}{6}\right), \tag{34}$$

$$\theta = y - \frac{\Gamma C^2}{4}\left(\frac{y^4}{3} - \frac{2y^3}{3} + \frac{y^2}{2} - \frac{y}{6}\right)$$

$$+ \Lambda\Gamma C^4\left(\frac{y^6}{15} - \frac{y^5}{5} + \frac{y^4}{4} - \frac{y^3}{6} + \frac{y^2}{16} - \frac{y}{80}\right). \tag{35}$$

It is well-known from the perturbation theory that the correction terms must be much smaller than the leading terms for the solutions to be valid. Hence, the validity criterion of these two solutions is

$$Cr = 2\Lambda C^2 \ll 1. \tag{36}$$

It should be noted that this solution is equivalent to the second iteration of PIA(1,1) when $\varepsilon = 1$.

3.4 Comparisons With the Numerical Solution

In this section, for different values of the pressure gradient C, the non-Newtonian coefficient Λ and the Brinkman number Γ, solutions of the PIA(1,1), PIA(1,2), and the regular perturbation will be compared with each other as well as with the numerical solutions. The numerical solutions are calculated with Wolfram Mathematica's built-in command, NDSolve.

Figure 1 shows that all the solutions match well enough, when small values of the parameters satisfying the validity criterion are chosen, as expected. Especially, the non-Newtonian behaviour is assumed to be small in the calculations of Figure 1.

When the values of the parameters are increased further, the validity criterion does not hold anymore. The perturbation solution predicts backflow adjacent to the plates which are unphysical for a constant pressure drop between the plates (Fig. 2). The PIA(1,2) solution predicts the velocity profile better than the PIA(1,1) solution.

When the physical parameters are considerably larger and far beyond the validity criterion ($Cr=8$), the perturbation solution predicts a backflow within all the domain which is not correct at all (Fig. 3). The PIA(1,1) solution does not predict the velocity profiles quantitatively well with an exaggerated maximum velocity. The PIA(1,2) velocity profiles are in acceptable agreement with the numerical ones.

As far as the temperature profiles are considered, the matches are better among the solutions. For the criterion of 0.2, the temperatures are indistinguishable as shown in Figure 4. One reason might be that the first non-linear
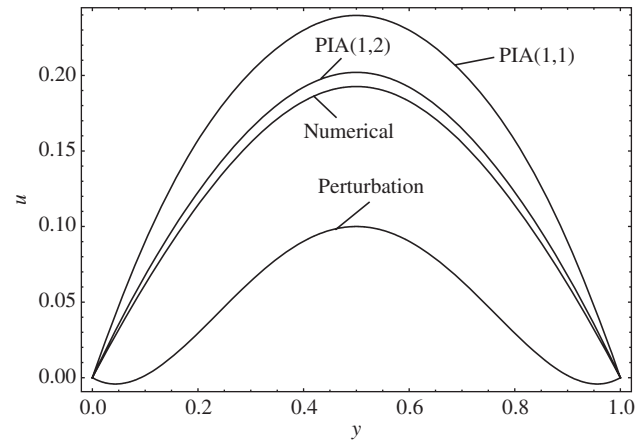

Figure 2: Comparison of the approximate velocity solutions with the numerical solution. $\varepsilon=1$, $C=-2$, $\Lambda=0.6$, $\Gamma=5$, $Cr=4.8$.
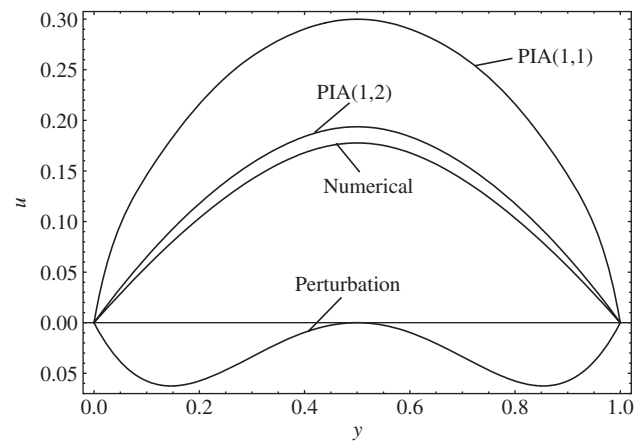

Figure 3: Comparison of the approximate velocity solutions with the numerical solution. $\varepsilon=1$, $C=-2$, $\Lambda=1$, $\Gamma=5$, $Cr=8$.
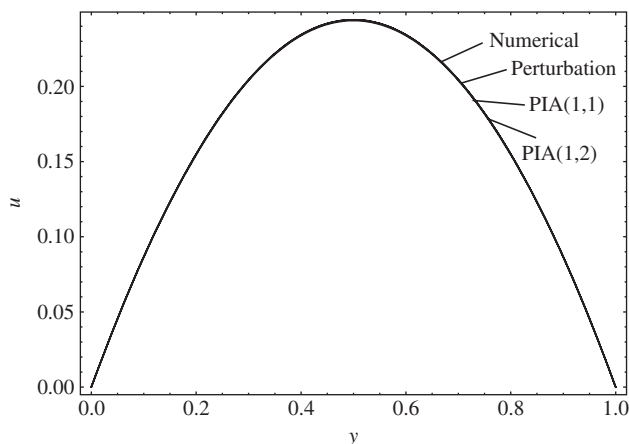

Figure 1: Comparison of the approximate velocity solutions with the numerical solution. $\varepsilon=1$, $C=-2$, $\Lambda=0.025$, $\Gamma=5$, $Cr=0.2$.
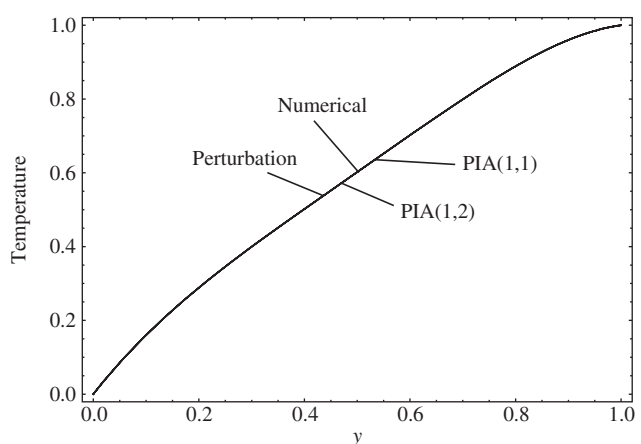

Figure 4: Comparison of the approximate temperature solutions with the numerical solution. $\varepsilon=1$, $C=-2$, $\Lambda=0.025$, $\Gamma=5$, $Cr=0.2$.

term involving only the Brinkman number is taken as an $O(1)$ term in the energy equation, i.e. (11).

In Figure 5, the perturbation and the PIA(1,1) solutions start diverging as the criterion gets larger. PIA(1,1) seems to perform slightly better than the perturbation solution. PIA(1,2), on the other hand, agrees well with the numerical solution. Nevertheless, all the solutions are within the acceptable percentage error.

The last case for the temperature solutions are presented in Figure 6. The criterion is 8, a fairly large number compared to 1. The perturbation and the PIA(1,1) solutions diverge from the numerical solution while the PIA(1,2) solution still matches with the numerical solution reasonably. For this specific case, the perturbation solution performed slightly better than the PIA(1,1) solution.

In addition to the comparisons of the velocity and temperature profiles, the comparisons of the dimensionless

Figure 5: Comparison of the approximate temperature solutions with the numerical solution. $\varepsilon = 1$, $C = -2$, $\Lambda = 0.6$, $\Gamma = 5$, $Cr = 4.8$.
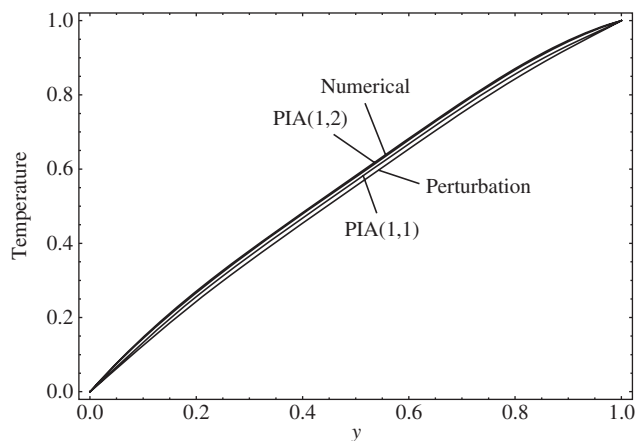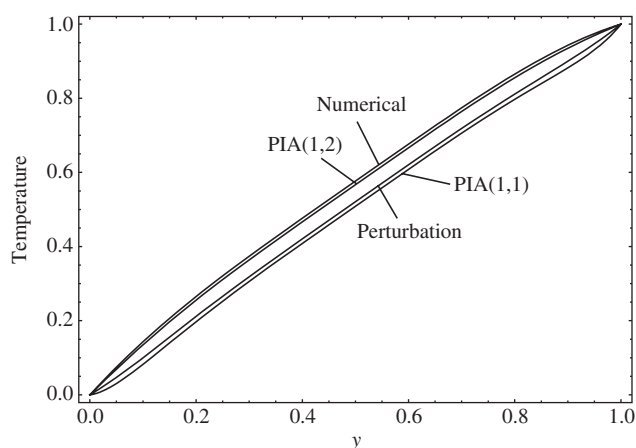

Figure 6: Comparison of the approximate temperature solutions with the numerical solution. $\varepsilon = 1$, $C = -2$, $\Lambda = 1$, $\Gamma = 5$, $Cr = 8$.

shear stress and the Nusselt number are also given since these dimensionless parameters are technologically important. The dimensionless equation defining the shear stress of a third-grade fluid is

$$\tau_{xy} = \frac{du}{dy} + 2\Lambda \left(\frac{du}{dy}\right)^3 \qquad (37)$$

where u is the dimensionless velocity and Λ is the dimensionless parameter related to the non-Newtonian behaviour as defined before. The dimensionless shear stress is related to the dimensional one (with over tilde) as follows

$$\tau_{xy} = \frac{\tilde{\tau}_{xy}}{\dfrac{\mu_* V}{h}}. \qquad (38)$$

Using (37), Table 1 is computed for the comparison of the shear stresses calculated by the numerical and approximate solutions for different non-Newtonian parameter values.

An interesting feature in the numerical results is that the shear stresses remained almost unchanged by the increase in the non-Newtonian parameter. Increasing Λ decreases the slope of the velocity due to the non-Newtonian effects and their combination in the stress equation produces similar values. However, approximate solutions give diverging results near boundaries as Λ increases. This is due to the higher slopes of the approximate solutions than the numerical ones near the boundaries as it can

Table 1: Comparison of the dimensionless shear stresses along the y-axis ($\varepsilon = 1$, $\mu = 1$, $C = -2$, $\Gamma = 5$).

Λ	y	Numerical	PIA(1,1)	PIA(1,2)	Perturbation
0.025	0	1.000000	1.000973	1.000279	0.992869
	0.2	0.599999	0.600030	0.600009	0.599427
	0.4	0.199999	0.200000	0.200000	0.199998
	0.6	−0.199999	−0.200000	−0.200000	−0.199998
	0.8	−0.599999	−0.600030	−0.600009	−0.599427
	1	−1.000000	−1.000973	−1.000279	−0.992869
0.6	0	0.999999	2.244493	1.223687	−0.209599
	0.2	0.599999	0.754888	0.625802	0.388299
	0.4	0.200000	0.200173	0.200049	0.198683
	0.6	−0.200000	−0.200173	−0.200049	−0.198683
	0.8	−0.599999	−0.754888	−0.625802	−0.388299
	1	−0.999999	−2.244493	−1.223687	0.209599
1	0	0.999999	57	1.443149	−3
	0.2	0.599999	1.00235	0.662172	0.177483
	0.4	0.200000	0.200733	0.200195	0.196459
	0.6	−0.200000	−0.200733	−0.200195	−0.196459
	0.8	−0.59999	−1.00235	−0.662172	−0.177483
	1	−0.999999	−57	−1.443149	3

also be verified visually from the graphs. The shear stress decreases as y is increased till the midline where the flow reaches its maximum speed and the lowest value of shear stress is observed there. When the three approximate solutions are compared, PIA(1,2) complies best with the numerical results.

For the heat transfer, the local Nusselt number is important

$$\mathrm{Nu} = \frac{\tilde{q}h}{k(\theta_2 - \theta_1)} = \frac{\mathrm{d}\theta}{\mathrm{d}y}, \tag{39}$$

where $\tilde{q}$ denotes the heat flux and the rest of the parameters are the same as defined in (12).

The Nusselt number and consequently the heat transfer rate decrease as we get closer to the upper plate (Table 2). PIA(1,2) solutions are closer to the numerical ones than the other solutions. As the non-Newtonian coefficient increases, the Nusselt numbers in the lower mid-part decrease, but a slight increase is observed for the upper mid-part.

In conclusion, for the velocity profiles, all solutions are in reasonable agreement within the range of validity of the perturbation solution. Beyond the range of validity, the PIA solutions agree better with the numerical ones and the PIA(1,2) performs better than the PIA(1,1). The perturbation solution, however, is not reliable as it gives quantitatively and qualitatively wrong behaviour for velocities if the criterion is not satisfied. For the temperature profiles, the qualitative behaviour is the same for all solutions although there are some small variations in the results quantitatively. For temperature profiles, the best agreement is observed for PIA(1,2). In conclusion, for non-Newtonian fluids, the perturbation iteration algorithms may be used to find approximate analytical solutions at least for some simple flow geometries.

Table 2: Comparison of the local Nusselt numbers along the y-axis ($\varepsilon = 1, \mu = 1, C = -2, \Gamma = 5$).

Λ	y	Numerical	PIA(1,1)	PIA(1,2)	Perturbation
0.6	0	1.616054	1.302758	1.554431	1.233333
	0.2	1.153189	1.153724	1.151650	1.133340
	0.4	1.006492	1.006493	1.006492	1.006475
	0.6	0.993508	0.993507	0.993508	0.993525
	0.8	0.846811	0.846276	0.848349	0.866656
	1	0.383946	0.697242	0.445569	0.766667
1	0	1.562657	0.177323	1.415282	0.833333
	0.2	1.143772	1.132576	1.138883	1.102239
	0.4	1.006391	1.006395	1.006391	1.006346
	0.6	0.993609	0.993605	0.993609	0.993653
	0.8	0.856228	0.867424	0.861117	0.897769
	1	0.437343	1.822677	0.584718	1.166667

4 Parallel Plate Flow of a Newtonian Fluid With Temperature-Dependent Viscosity

Although the fluid model is Newtonian and simpler in this case, the dependence of the viscosity on the temperature introduces further nonlinearities and makes the momentum and energy equations coupled. The steady-state equations and the boundary conditions are

$$\frac{\mathrm{d}\mu}{\mathrm{d}y}\frac{\mathrm{d}u}{\mathrm{d}y} + \mu\frac{\mathrm{d}^2u}{\mathrm{d}y^2} = C \quad u(0)=0, \; u(1)=0, \tag{40}$$

$$\frac{\mathrm{d}^2\theta}{\mathrm{d}y^2} + \varepsilon\Gamma\mu\left(\frac{\mathrm{d}u}{\mathrm{d}y}\right)^2 = 0 \quad \theta(0)=0, \; \theta(1)=1, \tag{41}$$

where u is the dimensionless velocity, θ is the dimensionless temperature, and μ is the dimensionless viscosity. The dimensionless parameters are defined in terms of the dimensional ones as

$$y = \frac{\tilde{y}}{h}, \; \theta = \frac{\tilde{\theta} - \theta_1}{\theta_2 - \theta_1}, \; u = \frac{\tilde{u}}{V}, \; \mu = \frac{\tilde{\mu}}{\mu_*}, \tag{42}$$

where h is the distance between the parallel plates, θ_1 and θ_2 are the temperatures of the bottom and top plates, respectively, V is the reference velocity, and μ_* is the reference viscosity. The dimensionless physical parameters are

$$C = \frac{C_1 h^2}{\mu_* V}, \; C_1 = \frac{\mathrm{d}p}{\mathrm{d}x}, \; \Gamma = \frac{\mu_* V^2}{k(\theta_2 - \theta_1)}, \tag{43}$$

where C_1 is the constant pressure drop in the axial direction, C is the dimensionless pressure drop parameter, and Γ is the Brinkman number. For this problem, the viscosity is an exponentially decaying function of the temperature

$$\mu = e^{-\varepsilon m\theta}, \tag{44}$$

which is called the Reynolds model. For $m = 0$, $\mu = 1$ and the model reduces to the constant viscosity case. ε is introduced artificially in the coefficient of the nonlinear term in the energy equation and also as a coefficient in front of the viscosity decay parameter. It can be taken as 1 at the end of the calculations.

4.1 Perturbation-Iteration Algorithm PIA(1,1)

Substituting the Reynolds model viscosity into the problem, (40) and (41) are rewritten in the following form:

$$F_1(u'', u', \theta', \theta, \varepsilon) = -\varepsilon m\theta' u' e^{-\varepsilon m\theta} + e^{-\varepsilon m\theta} u'' - C = 0, \quad (45)$$

$$F_2(\theta'', \theta, u', \varepsilon) = \theta'' + \varepsilon\Gamma e^{-\varepsilon m\theta}(u')^2 = 0. \quad (46)$$

One correction term perturbation expansions are substituted into (45) and (46) and then expanded in Taylor series with first-order derivatives. The following equations of iteration are obtained as a result

$$u_n''' - C + \varepsilon(u_c)_n'' - \varepsilon m\theta_n' u_n' - \varepsilon m\theta_n u_n'' = 0, \quad (47)$$

$$\varepsilon(\theta_c)_n'' + \theta_n'' + \varepsilon\Gamma(u_n')^2 = 0. \quad (48)$$

Simple initial functions that satisfy the boundary conditions can be selected as

$$u_0 = 0, \quad (49)$$

$$\theta_0 = y. \quad (50)$$

The first iteration solutions are then

$$u_1 = \frac{C}{2}(y^2 - y), \quad (51)$$

$$\theta_1 = y. \quad (52)$$

Finally, the second and third iteration solutions are calculated

$$u_2 = \frac{C}{2}(y^2 - y) + \varepsilon mC\left(\frac{y^3}{3} - \frac{y^2}{4} - \frac{y}{12}\right), \quad (53)$$

$$\theta_2 = y + \varepsilon C^2\Gamma\left(-\frac{y^4}{12} + \frac{y^3}{6} - \frac{y^2}{8} + \frac{y}{24}\right), \quad (54)$$

$$u_3 = \frac{C}{2}(y^2 - y) + \varepsilon mC\left(\frac{y^3}{3} - \frac{y^2}{4} - \frac{y}{12}\right) + \varepsilon^2 m^2 C\left(\frac{y^4}{4} - \frac{y^3}{6} - \frac{y^2}{24} - \frac{y}{24}\right)$$
$$+ \varepsilon^2 m\Gamma C^3\left(-\frac{y^6}{72} + \frac{y^5}{24} - \frac{5y^4}{96} + \frac{5y^3}{144} - \frac{y^2}{96}\right)$$
$$+ \varepsilon^3 m^2\Gamma C^3\left(-\frac{y^7}{84} + \frac{5y^6}{144} - \frac{29y^5}{720} + \frac{13y^4}{576} - \frac{y^3}{288} - \frac{y^2}{576} + \frac{y}{10080}\right), \quad (55)$$

$$\theta_3 = y + \varepsilon C^2\Gamma\left(-\frac{y^4}{12} + \frac{y^3}{6} - \frac{y^2}{8} + \frac{y}{24}\right)$$
$$+ \varepsilon^3 m^2 C^2\Gamma\left(-\frac{y^6}{30} + \frac{y^5}{20} - \frac{y^4}{144} - \frac{y^3}{72} - \frac{y^2}{288} + \frac{11y}{1440}\right)$$
$$+ \varepsilon^2 mC^2\Gamma\left(-\frac{y^5}{10} + \frac{y^4}{6} - \frac{y^3}{18} - \frac{y^2}{24} + \frac{11y}{360}\right). \quad (56)$$

Note again that the PIA(1,1) solutions are of polynomial type.

4.2 Perturbation-Iteration Algorithm PIA(1,2)

The iteration equations of PIA(1,2) are found by first substituting the perturbation expansions with one correction terms into (40) and (41) and then expanding in Taylor series up to second-order derivatives

$$F_1 \cong u_n'' - C + \varepsilon(-m\theta_n' u_n' - m\theta_n u_n'' + (u_c'')_n)$$
$$+ \frac{\varepsilon^2}{2}(2m^2\theta_n' u_n'\theta_n + m^2\theta_n^2 u_n'' - 2m\theta_n(u_c'')_n - 2m\theta_n'(u_c')_n$$
$$- 2mu_n'(\theta_c')_n - 2mu_n''(\theta_c)_n) = 0 \quad (57)$$

$$F_2 \cong \theta_n'' + \varepsilon(\Gamma(u_n')^2 + (\theta_c'')_n) + \frac{\varepsilon^2}{2}(4\Gamma u_n'(u_c')_n - 2m\Gamma\theta_n(u_n')^2) = 0. \quad (58)$$

Starting with the same initial guesses as in the previous section

$$u_0 = 0, \quad (59)$$

$$\theta_0 = y, \quad (60)$$

the first iteration solutions are found as

$$u_1 = \frac{C}{m\varepsilon}\left(-y + \frac{\ln[1 - my\varepsilon]}{\ln[1 - m\varepsilon]}\right), \quad (61)$$

$$\theta_1 = y. \quad (62)$$

From the definition of the logarithm, $\varepsilon m < 1$ must hold for the first iteration solutions to be valid. The next iteration is not calculated due to this limited validity of the solution and the complexities encountered in the equations.

4.3 Perturbation Solution

For the regular perturbation solution of the problem, expansions with two correction terms are taken into account

$$u = u_0 + \varepsilon u_1 + \varepsilon^2 u_2, \quad (63)$$

$$\theta = \theta_0 + \varepsilon\theta_1 + \varepsilon^2\theta_2. \quad (64)$$

Reynolds model of viscosity is also expanded in a series

$$\mu = 1 - \varepsilon m(\theta_0 + \varepsilon\theta_1 + \varepsilon^2\theta_2) + \frac{\varepsilon^2 m^2}{2}(\theta_0 + \varepsilon\theta_1 + \varepsilon^2\theta_2)^2. \quad (65)$$

Substituting these expansions into (40) and (41) and separating at each order of approximation, one will have three sets of equations to be solved consecutively both for the velocity and temperature profiles. The equations at each order are solved and the solutions are substituted into the perturbation expansions. Thus, the two term perturbation solutions for the problem are

$$u = \frac{C}{2}(-y + y^2) + \varepsilon\left[\frac{Cm}{12}(-y - 3y^2 + 4y^3)\right]$$
$$\varepsilon^2\left[m^2 C\left(-\frac{y^2}{24} - \frac{y^3}{12} + \frac{y^4}{8}\right)\right.$$
$$\left. + mC^3\Gamma\left(-\frac{y^2}{96} + \frac{5y^3}{144} - \frac{5y^4}{96} + \frac{y^5}{24} - \frac{y^6}{72}\right)\right], \quad (66)$$

$$\theta = y + \varepsilon\left[\frac{C^2\Gamma}{24}(y - 3y^2 + 4y^3 - 2y^4)\right]$$
$$+ \varepsilon^2\left[mC^2\Gamma\left(\frac{y}{45} - \frac{y^2}{24} - \frac{y^3}{72} + \frac{y^4}{12} - \frac{y^5}{20}\right)\right]. \quad (67)$$

Imposing the condition that each correction term be much smaller than the previous term, the validity criteria are

$$Cr_1 = \frac{2\varepsilon m}{3} \ll 1, \quad Cr_2 = \frac{\varepsilon C^2 \Gamma}{6} \ll 1. \quad (68)$$

The first criterion involves the viscosity decaying parameter and the second criterion involves a combination of the pressure drop as well as the Brinkman number.

4.4 Comparisons With the Numerical Solution

In this section, solutions of the PIA(1,1), PIA(1,2), and the regular perturbation will be compared with each other as well as with the numerical solutions for different values of the pressure drop, the viscosity parameter, and the Brinkman number. The numerical solutions are calculated with Wolfram Mathematica's built-in command, NDSolve.

In Figure 7, the PIA(1,1) and the PIA(1,2) solutions are in good agreement with the numerical solution, while there is a small discrepancy for the perturbation solution especially at the fully developed flow region. Despite the fact that only the first criterion is satisfied, the perturbation solution does not introduce much error.

In Figure 8, due to the increase in the viscosity parameter, the curves bent to the right and the maximum
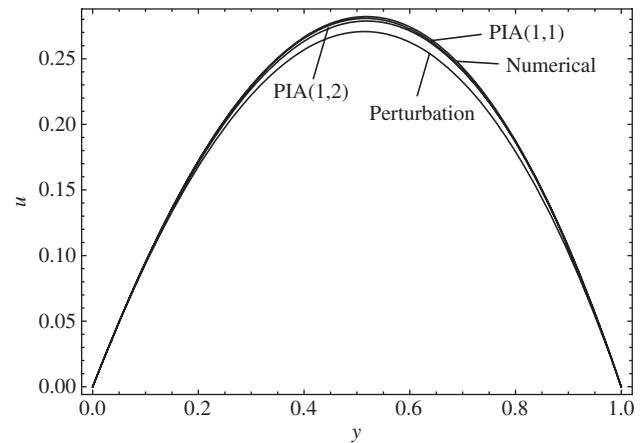
Figure 7: Comparison of the approximate velocity solutions with the numerical solution. $\varepsilon = 1$, $m = 0.2$, $C = -2$, $\Gamma = 5$, $Cr_1 = 0.13$, $Cr_2 = 3.33$.
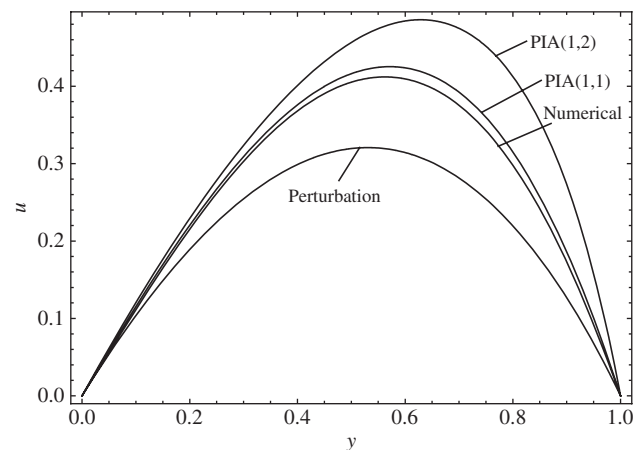
Figure 8: Comparison of the approximate velocity solutions with the numerical solution. $\varepsilon = 1$, $m = 0.8$, $C = -2$, $\Gamma = 5$, $Cr_1 = 0.53$, $Cr_2 = 3.33$.

velocities occur closer to the upper plate where the temperature is greater compared to the lower one. The closest approximate solution to the numerical one is the PIA(1,1) solution. Since m is large and the PIA(1,2) solution consists of a logarithmic function for which $\varepsilon m < 1$ condition must hold, the solution over-predicts the location and magnitude of the maximum velocity.

Figure 9 shows the comparison of the approximate solutions for $m = 1.1$. Only the PIA(1,1) and the perturbation solutions are plotted here, as this is an undefined region for the PIA(1,2) solution. The perturbation solution under-predicts the location and magnitude of the maximum velocity. However, PIA(1,1) solution still remains close to the numerical one.
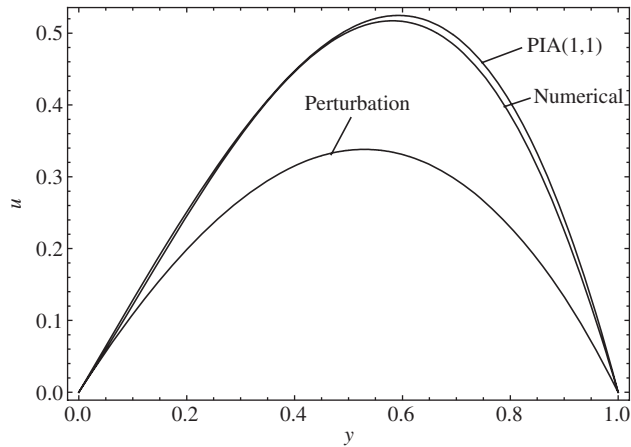
Figure 9: Comparison of the approximate velocity solutions with the numerical solution. $\varepsilon = 1$, $m = 1.1$, $C = -2$, $\Gamma = 5$, $Cr_1 = 0.73$, $Cr_2 = 3.33$.
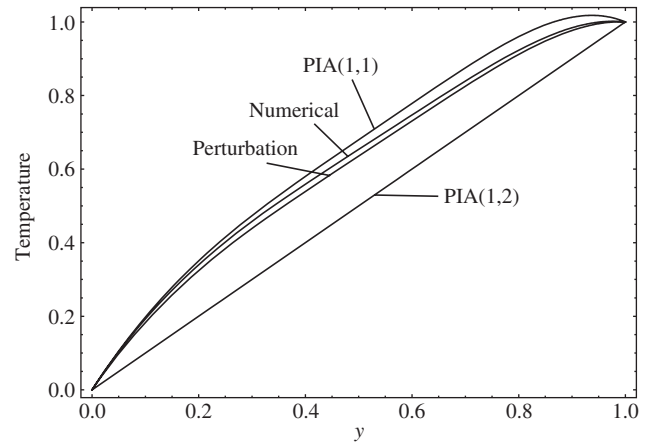

Figure 11: Comparison of the approximate temperature solutions with the numerical solution. $\varepsilon = 1$, $m = 0.6$, $C = -2$, $\Gamma = 5$, $Cr_1 = 0.4$, $Cr_2 = 3.33$.

Regarding the temperature profiles, the PIA(1,1) and the perturbation solution matches well with the numerical solution in the case where one of the criteria is not satisfied (Fig. 10). On the other hand, the first iteration solution of PIA(1,2) being $\theta_1 = y$ is a rough estimation and differs from the others.

When the viscosity parameter m is increased, it is observed from Figure 11 that the solutions begin diverging. Here, the perturbation solution performed relatively better than PIA(1,1) especially in the region near the upper plate.

The last case where $m = 1.1$ is presented in Figure 12. Both criterion are higher than should be for a regular solution, and hence, the perturbation solution is further away from the numerical solution when compared with PIA(1,1) which agrees quite well up to $y = 0.4$ and gradually diverges as y increases.
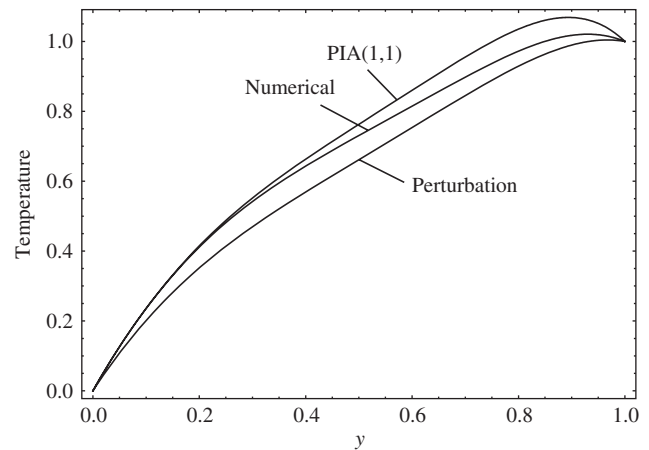

Figure 12: Comparison of the approximate temperature solutions with the numerical solution. $\varepsilon = 1$, $m = 1.1$, $C = -2$, $\Gamma = 5$, $Cr_1 = 0.73$, $Cr_2 = 3.33$.

Similar to the previous problem, the shear stresses and the Nusselt numbers of the flow along the y-axis will be contrasted. The dimensionless shear stress equation of the steady-state parallel plate flow of a Newtonian fluid is

$$\tau_{xy} = \mu \frac{du}{dy}, \tag{69}$$

with the dimensionless parameters defined in (12) and (38). Substituting the Reynolds model of viscosity into (69), the shear stress equation takes the below form

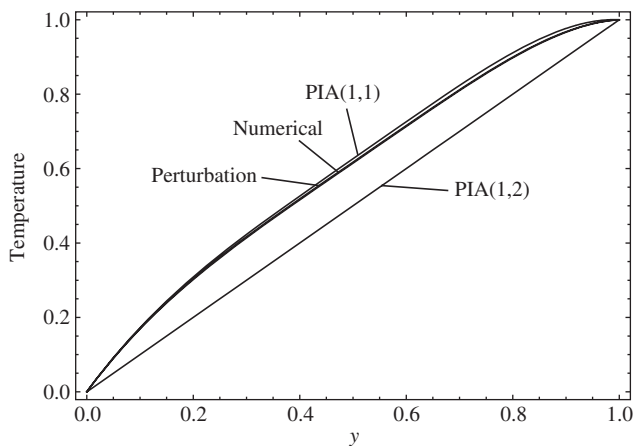$$\tau_{xy} = e^{-m\theta} \frac{du}{dy}. \tag{70}$$

Figure 10: Comparison of the approximate temperature solutions with the numerical solution. $\varepsilon = 1$, $m = 0.2$, $C = -2$, $\Gamma = 5$, $Cr_1 = 0.13$, $Cr_2 = 3.33$.

In Table 3, the shear stress values slightly increase as m gets larger. When the approximate results are compared, with few exceptions, the shear stress values calculated by PIA(1,1) comply better to the numerically calculated ones than the other methods.

The Nusselt number for the steady-state parallel plate flow of a Newtonian fluid with temperature-dependent viscosity is defined as

$$Nu = \frac{\tilde{q}h}{k(\theta_2 - \theta_1)} = \frac{d\theta}{dy}, \qquad (71)$$

where $\tilde{q}$ is the heat flux. Table 4 is given for the comparison of the Nusselt numbers calculated by the different methods.

In Table 4, it is shown that increasing m has increased the Nusselt number in the region near the lower plate while decreasing it near the upper plate. When the Nusselt number is tracked along the y-axis for a fixed m value, it seems to decrease as we get close to the upper plate. In the table, PIA(1,2) is not presented as its first iteration solution is a rough estimation and the second iteration cannot be calculated due to a singularity in the velocity profile. When the other two approximate solutions are compared, both produce reasonable approximations to the numerical data with few exceptions.

Consequently, for the velocity profiles, all solutions agree well with each other when the validity criteria are satisfied. Exceeding the limit of the criteria, solutions start to diverge with perturbation solution inheriting too much error. In addition to that PIA(1,2) solutions agree well for the small values of the viscosity parameter m; however, they diverge due to the criterion caused by the logarithmic function as m gets larger. In general, the PIA(1,1) gives the most reliable results for the velocity profiles for the case

Table 3: Comparison of the shear stresses along the y-axis ($\varepsilon = 1$, $C = -2$, $\Gamma = 5$).

m	y	Numerical	PIA(1,1)	PIA(1,2)	Perturbation
0.2	0	1.032986	1.036508	1.037159	1.033333
	0.2	0.632987	0.634332	0.637684	0.606880
	0.4	0.232987	0.235495	0.237963	0.218159
	0.6	−0.167013	−0.164612	−0.164121	−0.163940
	0.8	−0.567013	−0.567986	−0.570977	−0.542711
	1	−0.967013	−0.979878	−0.985384	−0.944269
0.8	0	1.124712	1.184127	1.257330	1.133333
	0.2	0.724712	0.723869	0.869724	0.578785
	0.4	0.324712	0.333863	0.488367	0.210891
	0.6	−0.075288	−0.056265	0.068221	−0.103451
	0.8	−0.475288	−0.463573	−0.501909	−0.369055
	1	−0.875288	−0.965701	−1.66852	−0.653025

Table 4: Comparison of the local Nusselt numbers along the y-axis ($\varepsilon = 1$, $C = -2$, $\Gamma = 5$).

M	y	Numerical	PIA(1,1)	Perturbation
0.2	0	1.939028	1.961667	1.922222
	0.2	1.211579	1.230780	1.204622
	0.4	0.994709	1.008970	0.995289
	0.6	0.978488	0.991812	0.980622
	0.8	0.803331	0.793469	0.808622
	1	0.072784	−0.059444	0.088889
0.6	0	2.201195	2.255000	2.100000
	0.2	1.301565	1.354886	1.253867
	0.4	0.966530	1.017268	0.972533
	0.6	0.934261	0.985506	0.955199
	0.8	0.755545	0.731087	0.785867
	1	0.163626	−0.601667	−0.066667
1.1	0	2.684067	2.690417	2.322222
	0.2	1.504344	1.552292	1.315422
	0.4	0.922851	1.034557	0.944089
	0.6	0.837894	0.971505	0.923422
	0.8	0.644476	0.635637	0.757422
	1	−0.627251	−1.448194	−0.261111

of Newtonian flow. Calculating PIA(1,1) up to third iteration may be the significant cause, while due to limitations, PIA(1,2) algorithm is terminated at the first iteration. For the temperature profiles, PIA(1,1) and the perturbation solutions give similar results. If the criteria are too large, then the perturbation solution ceases to be valid.

The solutions of the previous section and this section can only be contrasted for the limiting cases of $\Lambda = 0$ when the non-Newtonian parameter vanishes. Both PIA(1,1) and PIA(1,2) solutions given in (25) and (33) reduce to

$$u = \frac{C}{2}(y^2 - y). \qquad (72)$$

For (33), when Λ approaches zero, the singularity should be removed by the L'Hopital's rule. The above solution can also be retrieved for the Newtonian fluid with Reynolds model parameter $m = 0$. For $m = 0$ in (55) and (66), (72) is obtained.

5 Conclusions

In this study, the perturbation-iteration algorithms are applied to the flow of a third-grade fluid and to the flow of a Newtonian fluid with temperature-dependent viscosity. Two different perturbation-iteration algorithms are used. Results are then compared with the regular perturbation and the numerical solutions. The following conclusions can be made.

1. The perturbation-iteration algorithm solutions are better in terms of predicting the velocity profiles for the case of third-grade fluid flow. The regular perturbation solutions predict erroneous velocity profiles such as unphysical backflow when the validity criteria are not met.

2. In determining the temperature profiles in a third-grade fluid, the variations among the solutions are marginal and even the regular perturbation solutions predict the temperatures with acceptable errors beyond the validity criteria.

3. For the Newtonian flow with variable viscosity, the most reliable velocity and temperature profiles correspond to the PIA(1,1) solutions. PIA(1,2) did not produce better solutions than those of PIA(1,1) due to the termination of the iterations and due to the limitations of the logarithmic function. The regular perturbation solutions are better than the PIA(1,2) solutions especially in predicting the temperature profiles.

4. The perturbation-iteration algorithms in general produce acceptable results beyond the limits of the validity range of the regular perturbation solutions.

5. PIA(1,2) solutions are of functional type while PIA(1,1) solutions are of polynomial type.

6. Especially, for non-Newtonian fluids, analytical solutions are rare. It is shown that the perturbation iteration method is effective in constructing analytical solutions to complex fluid problems.

References

[1] A. H. Nayfeh, Introduction to Perturbation Techniques, John Wiley and Sons, New York 1981.

[2] H. Hu, J. Sound Vib. **269**, 409 (2004).

[3] M. Pakdemirli, M. M. F. Karahan, and H. Boyacı, Math. Comput. Appl. **14**, 31 (2009).

[4] J. I. Ramos, Appl. Math. Comput. **193**, 303 (2007).

[5] A. M. Wazwaz, Commun. Nonlinear Sci. Numer. Simulat. **16**, 3881 (2011).

[6] V. Marinca and N. Herisanu, Acta Mech. **184**, 231 (2006).

[7] H. Hu, J. Sound Vib. **298**, 1159 (2006).

[8] J. H. He, J. Sound Vib. **7**, 631 (2001).

[9] H. Hu, J. Sound Vib. **298**, 446 (2006).

[10] D. D. Ganji, S. Karimpour, and S. S. Ganji, Int. J. Mod. Phys. B **23**, 2469 (2009).

[11] M. Pakdemirli, Y. Aksoy, and H. Boyacı, Math. Comput. Appl. **16**, 890 (2011).

[12] M. Pakdemirli and H. Boyacı, Appl. Math. Comput. **184**, 783 (2007).

[13] M. Pakdemirli, H. Boyacı, and H. A. Yurtsever, Math. Comput. Appl. **12**, 117 (2007).

[14] M. Pakdemirli, H. Boyacı, and H. A. Yurtsever, Math. Comput. Appl. **13**, 123 (2008).

[15] Y. Aksoy and M. Pakdemirli, Comput. Math. Appl. **59**, 2802 (2010).

[16] Y. Aksoy and M. Pakdemirli, Int. J. Numer. Meth. H. **22**, 814 (2012).

[17] İ. Dolapci, M. Şenol, and M. Pakdemirli, J. Appl. Math. **2013**, 1 (2013).

[18] M. Şenol, İ. Dolapci, Y. Aksoy, and M. Pakdemirli, Abstr. Appl. Anal. **2013**, 1 (2013).

[19] M. Pakdemirli, J. Vib. Control (2015), in press.

[20] M. Pakdemirli, SpringerPlus **5**, 208 (2016). Doi: 10.1186/s40064-016-1859-4.

[21] A. Z. Szeri and K. R. Rajagopal, Int. J. Nonlinear Mech. **20**, 91 (1985).

[22] M. Yürüsoy, M. Pakdemirli, and B. S. Yılbaş, J. Mech. Eng. Sci. **222(4)**, 653 (2008).

[23] M. Ayub, A. Rasheed, and T. Hayat, Int. J. Eng. Sci. **41**, 2091 (2003).

[24] M. Massoudi and I. Christie, Int. J. Non-Linear Mech. **30**, 687 (1995).

[25] T. Hayat, A. H. Kara, and E. Momoniat, Int. J. Non-Linear Mech. **38**, 1533 (2003).

[26] R. Ellahi, M. Raza, and K. Vafai, Math. Comput. Model **55**, 1876 (2012).

[27] T. Hayat and A. H. Kara, Math. Comput. Model **43**, 132 (2006).

[28] O. A. Bég, M. J. Uddin, M. M. Rashidi, and N. Kavyani, J. Eng. Thermophys. **23(2)**, 79 (2014).

[29] M. M. Rashidi, M. T. Rastegari, M. Asadi, and O. Anwar Bég, Chem. Eng. Commun. **199**, 231 (2012).

[30] M. Keimanesh, M. M. Rashidi, Ali J. Chamkha, and R. Jafari, Comput. Math. Appl. **62**, 2871 (2011).